

Profilin2 is required for filamentous actin formation induced by human parainfluenza virus type 2

Keisuke Ohta, Yusuke Matsumoto, Machiko Nishio*

Department of Microbiology, School of Medicine, Wakayama Medical University, Japan



ARTICLE INFO

Keywords:

Human parainfluenza virus type 2
V protein
profilin2
Filamentous actin

ABSTRACT

We previously reported that human parainfluenza virus type 2 (hPIV-2) promoted RhoA activation and subsequent filamentous actin (F-actin) formation. Actin-binding proteins, such as profilin and cofilin, are involved in the regulation of F-actin formation by RhoA signaling. In the present study, we identified profilin2 as a key molecule that is involved in hPIV-2-induced F-actin formation. Immunoprecipitation assays demonstrated that hPIV-2 V protein binds to profilin2 but not to profilin1. Mutation of Trp residues within C-terminal region of V protein abolished the binding capacity to profilin2. Depletion of profilin2 resulted in the inhibition of hPIV-2-induced F-actin formation and the suppression of hPIV-2 growth. Overexpression of wild type V but not Trp-mutated V protein reduced the quantity of actin co-immunoprecipitated with profilin2. Taken together, these results suggest that hPIV-2 V protein promotes F-actin formation by affecting actin-profilin2 interaction through its binding to profilin2.

1. Introduction

Human parainfluenza virus type 2 (hPIV-2) is a non-segmented negative-strand RNA virus within the *Rubulavirus* genus of the *Paramyxoviridae* (Lamb and Parks, 2013). Its genome consists of six genes encoding the nucleocapsid (NP), phospho- (P), V, matrix (M), hemagglutinin-neuraminidase (HN), fusion (F), and large (L) proteins. P protein is produced by inserting two G nucleotides in P mRNA whereas V protein is a faithful transcript of P mRNA (Ohgimoto et al., 1990). Thus, N-terminal amino acid sequences of P and V proteins are in common. There are three Trp and seven Cys residues within the C-terminal V-specific region of V. These residues are important for V's activity against several host factors, including STATs (Nishio et al., 2005), AIP1/Alix (Nishio et al., 2007), TRAF6 (Kitagawa et al., 2013), tetherin (Ohta et al., 2016a), caspase1 (Ohta et al., 2018a), and inactive RhoA (Ohta et al., 2018b).

We previously reported that the hPIV-2 P and V proteins bind to Gα1, which leads to RhoA activation (Ohta et al., 2016b). Gα1 is a GTPase-activating protein for RhoA that converts GTP-bound active RhoA to GDP-bound inactive RhoA (Bos et al., 2007). There are many RhoA-dependent processes, including actin reorganization (Hall, 1998). Actin is a cytoskeletal protein that is present as either in a monomeric globular form (G-actin) or as polymeric filamentous actin (F-actin). We found that hPIV-2 infection causes F-actin formation through the

interaction of V protein with inactive RhoA (Ohta et al., 2018b). Both V- or P-Gα1 and V-inactive RhoA interactions seem to be a means of RhoA activation. However, it has not been identified how hPIV-2-induced RhoA activation causes F-actin formation. The G-actin/F-actin equilibrium is directly regulated by actin-binding proteins including profilins and cofilins, both of which act downstream of RhoA signaling (Carlier and Pantaloni, 1997; Watanabe et al., 1999).

Profilin is a small (12–17 kDa) actin-binding protein that promotes actin polymerization (Krishnan and Moens, 2009). It converts ADP-G-actin to ATP-G-actin by increasing the rate of adenine nucleotide exchange. The profilin-ATP-G-actin complex can interact with the barbed end of the actin filaments, followed by the dissociation of profilin. In mammals, four profilin isoforms (profilin1-4) have been reported. Profilin1 is universally present in all cell types and tissues (Witke et al., 1998), whereas the expression of profilin2 is tissue-specific with the highest expression in the brain (Di Nardo et al., 2000). Profilin2 is shown to be alternatively spliced into profilin2a and profilin2b (Di Nardo et al., 2000; Lambrechts et al., 2000). Profilin3 and profilin4 are restricted to the testes (Rust et al., 2012). Cofilin is another well-known actin-binding protein of 15–19 kDa (Bernstein and Bamburg, 2010; Kanellos and Frame, 2016). Cofilin preferably binds to ADP-actin at the pointed ends of the filaments, resulting in depolymerization of F-actin (Bernstein and Bamburg, 2010; Kanellos and Frame, 2016). In mammalian cells, cofilin has two isoforms; cofilin1 (non-muscle cofilin) and

* Corresponding author. Department of Microbiology, School of Medicine, Wakayama Medical University, 811-1, Kimiidera, Wakayama, 641-8509, Japan.
E-mail address: mnishio@wakayama-med.ac.jp (M. Nishio).

cofilin2 (muscle cofilin) (Ono et al., 1994; Bernstein and Bamburg, 2010). It is reported that several viruses regulate actin-binding proteins to promote growth. Profilin promotes RNA synthesis in respiratory syncytial virus (RSV) infections (Burke et al., 2000; Harpen et al., 2009). Cofilin is involved in virus assembly and budding of influenza A virus (Liu et al., 2014) and rabies virus (Zan et al., 2016). It is also important for ribonucleoprotein formation in measles virus (Koga et al., 2015).

In the present study, we hypothesized that actin-binding proteins such as profilins and cofilins are involved in hPIV-2-induced F-actin formation. To verify this, we investigated the interaction of these actin-binding proteins with hPIV-2 proteins. Furthermore, we examined the effects of these actin-binding proteins on F-actin formation and hPIV-2 growth.

2. Results

2.1. hPIV-2 V protein binds to profilin2 but not to profilin1

hPIV-2 infection promotes F-actin formation (Ohta et al., 2018b). There is a possibility that actin-binding proteins, profilin and cofilin are involved in hPIV-2-induced F-actin formation. Since hPIV-2 V and/or P proteins regulate RhoA activation and F-actin formation through their binding to GEF1 and RhoA (Ohta et al., 2016b, 2018b), we investigated whether these proteins interact with profilin and cofilin using immunoprecipitation. Among four profilin isoforms, we focused on profilin1 and profilin2 because it is unlikely that profilin3 and profilin4 with testis-specific expression (Rust et al., 2012) are involved in hPIV-2. COS cells were transfected with SR α encoding hPIV-2 V or P gene together with FLAG-tagged profilin1, profilin2, cofilin1, or cofilin2. None of these actin-binding proteins co-immunoprecipitated P protein (Fig. 1A, lanes 7–10). Among these actin-binding proteins, only profilin2 co-immunoprecipitated V protein (Fig. 1A, lane 3). A deletion mutant composed of only common regions of V and P proteins (V/P) could not bind to profilin2 (Fig. 1B, lane 4). These results indicate that the C-terminal V-specific region of V is important for its interaction with profilin2.

This region contains three Trp and seven Cys residues that are involved in V's functions against several host proteins (see Introduction). To test whether these residues affect profilin2 interaction, Cys-mutated (V_{C193/197A}, V_{C209/211/214A}, and V_{C218/221A}) and Trp-mutated V proteins (V_{W178H/W182E/W192A}) were subjected to immunoprecipitation assay. V_{W178H/W182E/W192A} lost its binding capacity to profilin2, while Cys mutations did not affect the interaction with profilin2 (Fig. 1B, lanes 5–8). Furthermore, NP-profilin2 interaction was not observed (Fig. 1B, lane 9).

2.2. Profilin2 knockdown inhibits hPIV-2-induced F-actin formation

hPIV-2 infection induces F-actin formation (Ohta et al., 2018b). To examine the effects of profilin2 on hPIV-2-induced F-actin formation, an HEK293 cell line knocked down for profilin2 (HEK293/profilin2 KD) was established. We confirmed the reduction of protein expression of profilin2 without affecting profilin1 expression (Fig. 2A). We examined F-actin distribution in HEK293/profilin2 KD using phalloidin. Profilin2 knockdown did not affect the amount of F-actin in mock-infected cells (Fig. 2B, ctrl and profilin2 KD, mock). In control cells (HEK293/ctrl), the amount of F-actin during hPIV-2 infection was 2- to 3-fold higher than mock-infected cells (Fig. 2B and C, ctrl, mock and hPIV-2), consistent with our previous finding (Ohta et al., 2018b). In contrast, profilin2 knockdown inhibited hPIV-2-induced F-actin formation (Fig. 2B and C, profilin2 KD, hPIV-2). It is reported that RSV infection causes F-actin formation (Bitko et al., 2003). To test whether the inhibition of F-actin formation by profilin2 knockdown is specific to hPIV-2, F-actin distribution in RSV-infected cells was observed. RSV infection into HEK293/ctrl increased in F-actin beneath the cellular

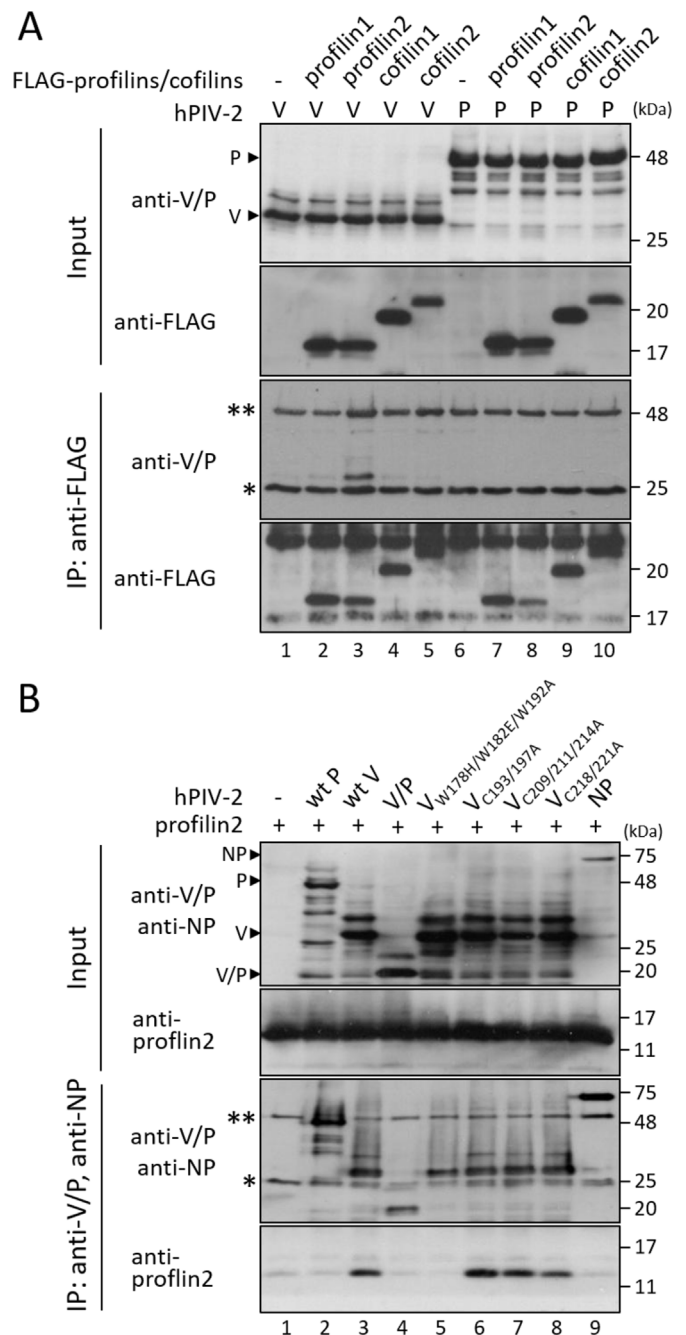


Fig. 1. Interaction between profilins and hPIV-2 proteins. COS cells in 12-well plates were transfected with various combinations of the indicated plasmids. After 48 h, cell lysates were analyzed directly by immunoblotting (input). Immunoprecipitates with anti-FLAG (A) or anti-V/P and anti-NP mAbs (B) were probed by anti-FLAG pAb, anti-V/P, anti-NP, and anti-profilin2 mAbs. Double and single asterisks indicate immunoglobulin heavy chain and light chain, respectively. All experiments were performed at least three times independently.

membrane rather than the long actin filament throughout the cells (Fig. 2B, ctrl, RSV). RSV-induced F-actin formation was not inhibited by profilin2 knockdown (Fig. 2B and C, profilin2 KD, RSV).

2.3. Profilin2 positively regulates hPIV-2 growth

To analyze the effects of profilin2 on hPIV-2 growth, HEK293/profilin2 KD was infected with hPIV-2 at an MOI of 0.1 or 1, and virus titers were evaluated by plaque assay. hPIV-2 growth in HEK293/profilin2 KD was five- to ten-fold lower (at an MOI of 1) and several

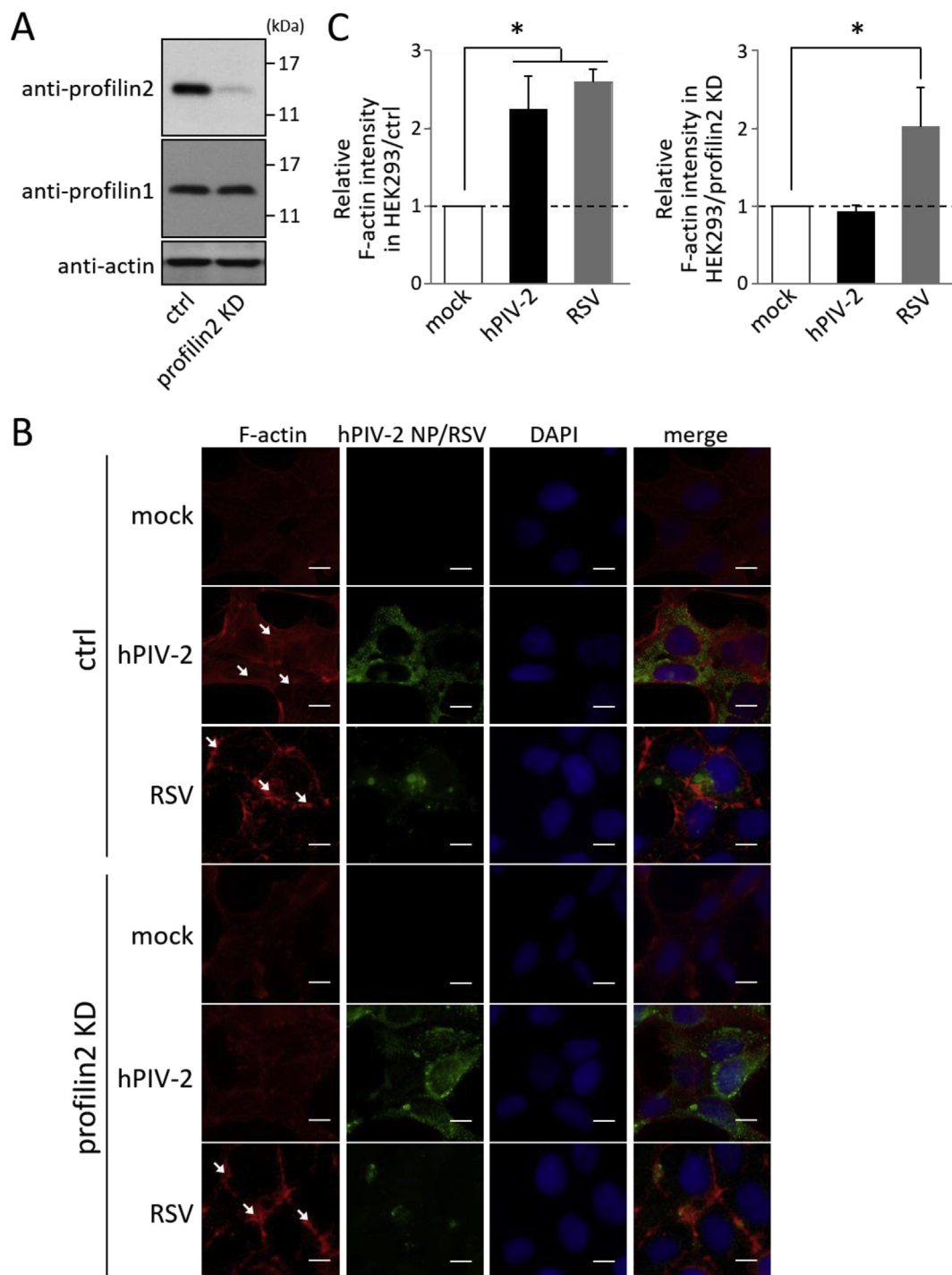


Fig. 2. The effects of profilin2 knockdown on F-actin distribution in virus-infected cells. (A) Cell lysates of profilin2-depleted HEK293 cell line (HEK293/profilin2 KD) and its control cells (HEK293/ctrl) were subjected to immunoblotting using anti-profilin2 mAb and anti-profilin1 pAb. Actin was used for a loading control. (B) HEK293/ctrl and HEK293/profilin2 KD were infected with or without hPIV-2 or RSV. After 48 h, cells were fixed, permeabilized, and stained with Acti-stain 555 phalloidin (red) and anti-NP mAb or FITC-labeled anti-RSV pAb (green). Nuclei were stained with DAPI (blue). The arrows indicate typical F-actin. Scale bar, 10 μ m. (C) Fluorescence intensity of F-actin was quantified using BZ-X Analyzer software (Keyence). The data are the means from three independent experiments, and are shown as the relative value (mock = 1). The *P* values were calculated by the Student's *t*-test. *, *P* < 0.05, compared to values of mock-infected cells. Error bars indicate standard deviations.

hundred-fold lower (at an MOI of 0.1) than that in HEK293/ctrl (Fig. 3A and B). We confirmed that hPIV-2 growth in the other two profilin2-depleted clones also showed lower than that in HEK293/ctrl (data not shown). To investigate whether profilin2 affects RSV growth, HEK293/profilin2 KD was infected with RSV at an MOI of 0.1, and virus titers were evaluated by CPE methods. Profilin2 knockdown did not affect

RSV growth (Fig. 3C). RSV growth in the other two profilin2-depleted clones was also similar to that in HEK293/ctrl (data not shown). These results indicate that profilin2 selectively promotes hPIV-2 growth.

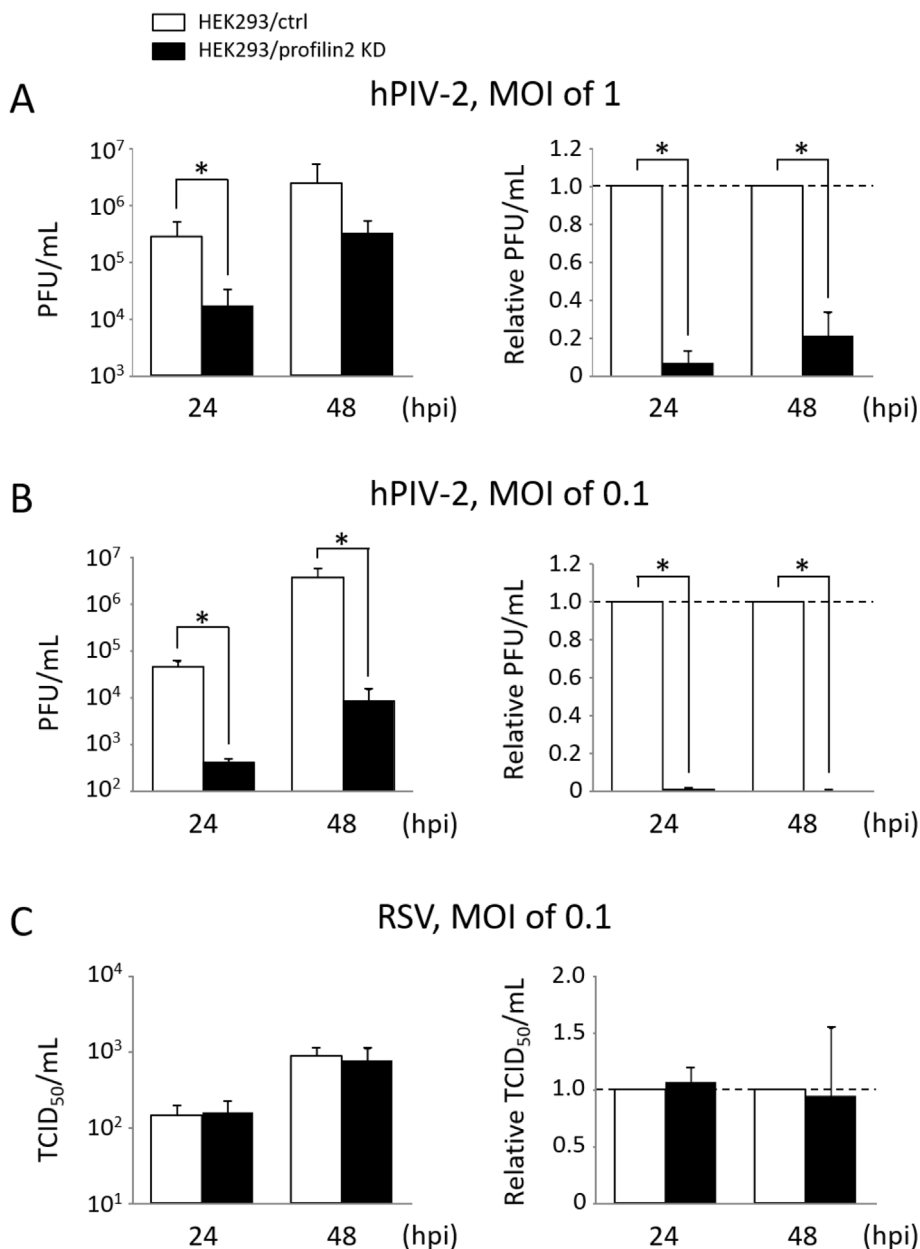


Fig. 3. Effects of profilin2 knockdown on hPIV-2 growth. (A and B) HEK293/profilin2 KD and HEK293/ctrl were infected with hPIV-2 at an MOI of 1 (A) or 0.1 (B) for the indicated hours, and titers were measured by plaque assay as described in the Materials and Methods section. The PFU counts are means from three independent experiments. *, $P < 0.05$, compared to values in control cells. (C) HEK293/profilin2 KD and HEK293/ctrl were infected with RSV at an MOI of 0.1 for the indicated hours, and titers were measured by CPE methods as described in the Materials and Methods section. TCID₅₀/mL values are means from three independent experiments. White and black bars indicate results from HEK293/ctrl and HEK293/profilin2 KD, respectively. Data are shown as the relative value (ctrl = 1). Error bars indicate standard deviations.

2.4. V protein attenuates actin-profilin2 interaction

V protein binds to profilin2 (Fig. 1), suggesting that V protein affects the profilin2 activity. Since profilin2 needs to bind to actin to regulate actin polymerization, we hypothesized that V protein is involved in actin-profilin2 interaction. To assess this possibility, immunoprecipitation assay of actin and profilin2 was performed in the absence or presence of V protein. HEK293 cells were transfected with FLAG-tagged profilin2 together with or without V. Endogenous actin was co-immunoprecipitated with FLAG-profilin2 (Fig. 4A, lane 2). In the presence of wild type (wt) V protein, the quantity of actin co-immunoprecipitated with FLAG-profilin2 decreased to approximately 70% relative to when wt V protein was absent (Fig. 4A, lane 3 and B). In contrast, V_{W178H/W182E/W192A} did not affect actin-profilin2 interaction (Fig. 4A, lane 4 and B). These results suggest that V protein attenuates actin-profilin2 interaction.

3. Discussion

hPIV-2 regulates RhoA signaling and actin polymerization through both the binding of its V and P proteins with Gaf1, and the binding of V with inactive RhoA (Ohta et al., 2016b, 2018b). In the present study, we identified profilin2 as a RhoA downstream molecule that is involved in hPIV-2-induced RhoA activation and F-actin formation.

We expected that V protein could bind to profilin1 since its expression is ubiquitous (Witke et al., 1998). However, V protein bound to profilin2 but not to profilin1 (Fig. 1). Profilin1 and profilin2 share 88% similarity in amino acid sequences, and their structures are almost superimposable (Nodelman et al., 1999), indicating that V protein can recognize minor and local differences in structure and/or amino acid residues between these isoforms. Alternatively, V-profilin2 interaction may be indirect via other protein(s). As shown in Fig. 2, profilin2 knockdown did not affect profilin1 expression level, and resulted in inhibition of hPIV-2-induced F-actin formation, indicating that profilin1 may not function as a mediator of actin polymerization induced by hPIV-2. Profilin1 is essential for cell survival, which is not

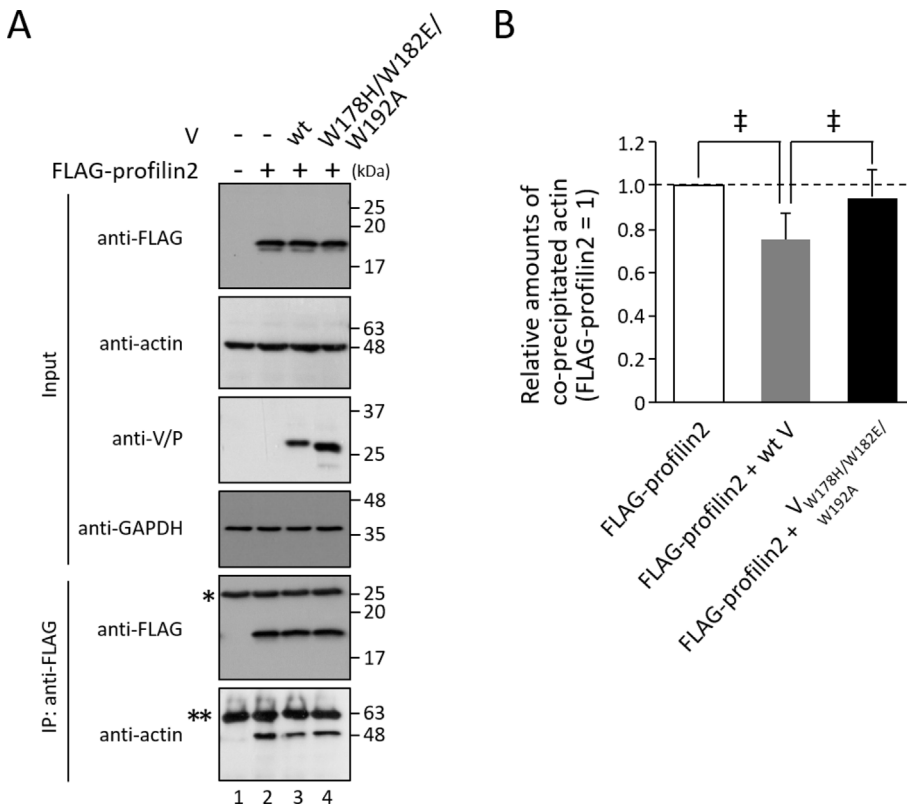


Fig. 4. Effects of V protein on the actin-profilin2 interaction. (A) HEK293 cells in six-well plates were transfected with FLAG-tagged profilin2 together with or without wt V or V_{W178H/W182E/W192A}. After 48 h, cell lysates were analyzed directly by immunoblotting (input). Immunoprecipitates with anti-FLAG mAb were probed by anti-actin, and anti-FLAG mAbs. Double and single asterisks indicate immunoglobulin heavy chain and light chain, respectively. (B) The bars show quantitative densitometry of immunoprecipitated actin analyzed using ImageJ software (<http://rsb.info.nih.gov/ij>). Signal intensity of immunoprecipitated actin was normalized by that of GAPDH. Data are the means from three independent experiments, and are shown as the relative value (FLAG-profilin2 = 1). †, $P < 0.05$, compared to values of FLAG-profilin2. Error bars indicate standard deviations.

compensated for by profilin2 (Witke et al., 2001). The reason why V protein regulates profilin2 but not profilin1 might be due to the avoidance of a lethal damage to the host cell.

We also found that V protein can affect actin-profilin2 interaction (Fig. 4). Amino acid residues in profilin that are important for the binding with actin have been identified (Schutt et al., 1993; Harpen et al., 2009), all of which are conserved in profilin1 and profilin2. Therefore, V protein does not seem to directly bind to these residues in profilin2. V-profilin2 interaction might cause conformational change of profilin2. Although profilin-G-actin interaction is important for the elongation of F-actin, profilin needs to dissociate from G-actin after attachment of G-actin to the barbed end of actin filament (Fig. 5). Profilin also interacts with phosphatidylinositol-4,5-bisphosphate (PIP₂), resulting in a rapid and efficient dissociation of profilin-G-actin (Lassing and Lindberg, 1985). Human profilin2 has lower affinity for PIP₂ than human profilin1 (Lambrechts et al., 2000), suggesting that profilin2-actin is less sensitive to dissociation by PIP₂ than profilin1-actin. V protein might compensate for the insufficient PIP₂-mediated dissociation through the binding with profilin2 (Fig. 5). F-actin is known to be insoluble in non-ionic detergent such as Triton X-100 (Berryman et al., 2004). The detergent contained in the lysis buffer used is non-ionic NP-40, indicating that actin co-immunoprecipitated with FLAG-profilin2 shown in Fig. 4 is originally exists as monomers. Therefore, reduction of the precipitated actin level represents attenuation of profilin2-actin interaction, supporting the model shown in Fig. 5. We previously demonstrated that the infection of recombinant PIV-2 encoding Trp-mutated V protein (rPIV-2/V_{W178H/W182E/W192A}) does not induce F-actin formation (Ohta et al., 2018b). Inability of this V mutant to interact with profilin2 might also contribute to failure in F-actin formation by rPIV-2/V_{W178H/W182E/W192A}.

There is very little investigation of virus-profilin interaction except for a few reports regarding RSV. RSV RNA synthesis is promoted by actin and profilin (Burke et al., 2000; Harpen et al., 2009). Harpen et al. (2009) proposed that actin and profilin form complexes with P and NP-RNA, and interacts with viral polymerase, which leads to promotion of

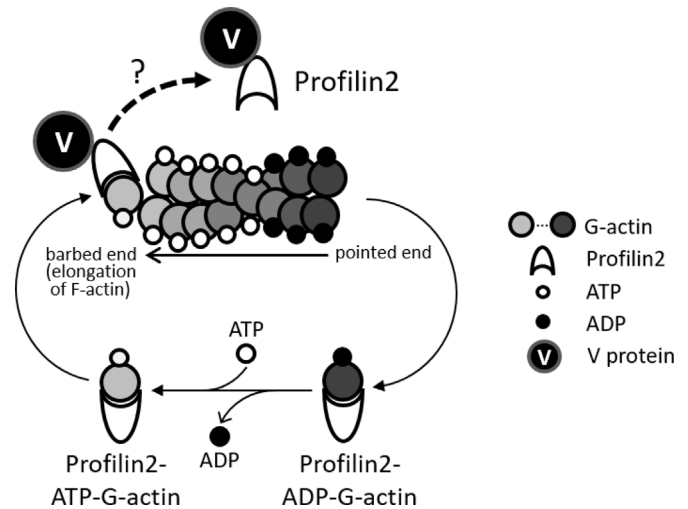


Fig. 5. Model for regulation of profilin2 by hPIV-2 V protein. Profilin2 binds to and converts ADP-G-actin to ATP-G-actin by increasing the rate of adenine nucleotide exchange. Profilin2-ATP-G-actin complex can interact with the barbed-end of F-actin, followed by the dissociation of profilin2 from G-actin. V protein potentially facilitates the dissociation of profilin2 from G-actin through the binding to profilin2.

polymerase activity. However, activation of viral transcription seems to be uninvolved in the actin polymerization since disruption of actin filaments does not affect viral transcription. F-actin formation by RSV infection occurs in HEp-2 and L2 but not in A549 cells, and F-actin formation does not affect viral growth (Bitko et al., 2003). In contrast, hPIV-2 growth closely correlates with F-actin formation (Figs. 2 and 3). These observations suggest that a mechanism how profilin and actin are involved in the viral lifecycle is different between hPIV-2 and RSV.

ROCK and mDia have been identified as RhoA effectors, and they cooperate during RhoA-induced actin reorganization (Watanabe et al.,

1999). mDia interacts with profilin-G-actin complex, followed by elongation of actin filament (Watanabe et al., 1997). Therefore, hPIV-2 seems to regulate mDia-dependent RhoA signals rather than ROCK-dependent signals, which is consistent with our previous finding that Y-27632, a ROCK-specific inhibitor, did not affect hPIV-2 growth (Ohta et al., 2016b).

Taken together with our previous reports, our results suggest that hPIV-2 tightly controls RhoA signaling and subsequent F-actin formation through binding of its V and/or P protein(s) to Gaf1, inactive RhoA, and profilin2. This triple regulation indicates that both RhoA activation and F-actin formation are essential for effective hPIV-2 growth.

4. Materials and methods

4.1. Cells and viruses

Vero cells were grown in Eagle's minimal essential medium (MEM) containing 10% fetal calf serum (FCS). A549, COS, HEK293 cells, and their derivatives were grown in Dulbecco's modified Eagle's MEM (DMEM) supplemented with 10% FCS. All cells were maintained in a humidified incubator at 37 °C with 5% CO₂. hPIV-2 (Toshiba strain) and RSV (Long strain) were used in this study.

4.2. Antibodies

Monoclonal antibodies (MAbs) against hPIV-2 V/P protein (315-1) and NP protein (159-1) were described previously (Nishio et al., 1997, 1999). Anti-Respiratory Syncytial Virus antibody (FITC) was purchased from Abcam (Cambridge, MA, USA). A polyclonal antibody (pAb) to profilin1 was obtained from Cell Signaling Technology (Danvers, MA, USA). MAb to profilin2 were purchased from Abnova (Taipei, Taiwan). Anti-FLAG mAb and pAb were obtained from Sigma (St. Louis, MO, USA). MAbs to actin and GAPDH were obtained from Wako (Osaka, Japan).

4.3. Plasmids

A pcDL-SRα296 vector carrying hPIV-2 V, P, NP, or their mutants was used (Nishio et al., 1996, 1997). cDNAs of profilin1 and profilin2 were obtained from A549 cell total RNA by reverse-transcription (RT)-PCR as described previously (Ohta et al., 2018c). Similarly, cofilin1 and cofilin2 cDNAs were obtained from HEK293 cell total RNA. These cDNAs were 100% identical to GenBank accession numbers NM_005022 (profilin1), NM_002628 (profilin2), BC011005 (cofilin1), and NM_021914 (cofilin2). These cDNAs were cloned into a pcDNA3.1/Hygro vector with FLAG tag at their N-termini (Invitrogen). Profilin2 cDNA was also cloned into a pEF4-Myc/His expression vector (Invitrogen, Carlsbad, CA). These constructs were all confirmed by DNA sequencing.

4.4. Establishment of profilin2 knockdown cell line

To deplete profilin2 expression, a DNA fragment encoding anti-profilin2 short hairpin RNA (shRNA) was cloned into a pHygH1dTO vector (Takei et al., 2006). The shRNA target sequence of profilin2 was 5'-CGCGAAGAAATGCTCAGTGAT-3' (corresponding to nucleotides 201–221 of the Profilin2 gene). HEK293 cells were transfected with pHygH1dTO carrying profilin2 shRNA using XtremeGENE HP. Stable transfectants were selected with 100 µg/ml hygromycin (Invitrogen). Clones with highly efficient depletion were used as profilin2 knockdown cells (HEK293/profilin2 KD). As a control, a cell line transduced with pHygH1dTO (an empty vector) was generated (HEK293/ctrl).

4.5. Immunoblot and immunoprecipitation assays

COS or HEK293 cells in 6-well or 12-well plates were transfected with plasmids encoding profilin1, profilin2, and/or various viral proteins using XtremeGENE HP (Roche, Basel, Switzerland) according to the manufacturer's instructions. At 48 h posttransfection, cells were harvested, sonicated for 30 s three times in lysis buffer containing 50 mM Tri-HCl pH 7.4, 150 mM NaCl, and 0.6% NP-40. Supernatants obtained by centrifugation were separated by SDS-PAGE, transferred to a nitrocellulose membrane, and analyzed by a Western blotting (WB) technique with the appropriate antibodies (Nishio et al., 2002). For immunoprecipitation, the supernatants were incubated with anti-V/P mAb and nProtein A Sepharose 4 Fast Flow (GE Healthcare Bio-Sciences, Piscataway, NJ, USA) for overnight at 4 °C (Nishio et al., 1996). Proteins were analyzed by WB technique. The protein signals were detected by chemiluminescence.

4.6. Immunofluorescence assay

HEK293 cells and their derivatives grown in 24-well plates were fixed with 4% paraformaldehyde. After being washed three times with phosphate-buffered saline (PBS), the cells were permeabilized with 0.2% Triton X-100 for 15 min. The cells were then incubated with appropriate antibodies. The secondary antibodies used were Alexa Fluor 488 goat anti-mouse IgG (Invitrogen). For the analyses of F-actin, Acti-Stain 555 Phalloidin (Cytoskeleton, Inc. Denver, CO, USA) was used. After being washed with PBS, the cells were analyzed with a fluorescence microscope, BZ-X700 (Keyence Co., Osaka, Japan). Fluorescence intensity of F-actin was quantified using the Hybrid Cell Count function of BZ-X Analyzer software (Keyence).

4.7. Virus growth kinetics

hPIV-2 growth was evaluated by plaque assay. Vero cells grown in 12-well plates were infected with viruses diluted serially 10-fold in MEM without FCS, and cultured in MEM containing 1.6% FCS and 1% SeaKem ME agarose (FMC BioProducts, Rockland, ME, USA). The cells were stained with 0.1% neutral red at 5 days post-infection (dpi), and the number of plaques was counted. RSV growth was evaluated by CPE methods. Vero cells grown in 24-well plates were infected with viruses diluted serially 10-fold in MEM without FCS, and cultured for 7 days. Titers were expressed as 50% tissue culture infection dose (TCID₅₀). TCID₅₀ was calculated using the Reed and Muench method (Reed and Muench, 1938).

Conflicts of interest

The authors declare that they have no competing interests.

Funding information

This work was supported by Grant-in-Aid Scientific Research from the Ministry of Education, Culture, Sports, Science and Technology, Japan (JP17K15703).

References

- Bitko, V., Oldenburg, A., Garmon, N.E., Barik, S., 2003. Profilin is required for viral morphogenesis, syncytium formation, and cell-specific stress fiber induction by respiratory syncytial virus. *BMC Microbiol.* 3, 9. <https://doi.org/10.1186/1471-2180-3-9>.
- Bernstein, B.W., Bamberg, J.R., 2010. ADF/cofilin: a functional node in cell biology. *Trends Cell Biol.* 20, 187–195. <https://doi.org/10.1016/j.tcb.2010.01.001>.
- Berryman, M., Bruno, J., Price, J., Edwards, J.C., 2004. CLIC-5A functions as a chloride channel in vitro and associates with the cortical actin cytoskeleton in vitro and in vivo. *J. Biol. Chem.* 279, 34794–34801. <https://doi.org/10.1074/jbc.M402835200>.
- Bos, J.L., Rehmann, H., Wittinghofer, A., 2007. GEFs and GAPs: critical elements in the control of small G proteins. *Cell* 129, 865–877. <https://doi.org/10.1016/j.cell.2007>.

- 05.018.
- Burke, E., Mahoney, N.M., Almo, S.C., Barik, S., 2000. Profilin is required for optimal actin-dependent transcription of respiratory syncytial virus genome RNA. *J. Virol.* 74, 669–675.
- Carlier, M.F., Pantaloni, D., 1997. Control of actin dynamics in cell motility. *J. Mol. Biol.* 269, 459–467. <https://doi.org/10.1006/jmbi.1997.1062>.
- Di Nardo, A., Gareus, R., Kwiatkowski, D., Witke, W., 2000. Alternative splicing of the mouse profilin II gene generates functionally different profilin isoforms. *J. Cell Sci.* 113, 3795–3803.
- Hall, A., 1998. Rho GTPases and the actin cytoskeleton. *Science* 279, 509–514.
- Harpen, M., Barik, T., Musiyenko, A., Barik, S., 2009. Mutational analysis reveals a noncontractile but interactive role of actin and profilin in viral RNA-dependent RNA synthesis. *J. Virol.* 83, 10869–10876. <https://doi.org/10.1128/JVI.01271-09>.
- Kanellos, G., Frame, M.C., 2016. Cellular functions of the ADF/cofilin family at a glance. *J. Cell Sci.* 129, 3211–3218. <https://doi.org/10.1242/jcs.187849>.
- Kitagawa, Y., Yamaguchi, M., Zhou, M., Nishio, M., Itoh, M., Gotoh, B., 2013. Human parainfluenza virus type 2 V protein inhibits TRAF6-mediated ubiquitination of IRF7 to prevent TLR7- and TLR9-dependent interferon induction. *J. Virol.* 87, 7966–7976. <https://doi.org/10.1128/JVI.03525-12>.
- Koga, R., Sugita, Y., Noda, T., Yanagi, Y., Ohno, S., 2015. Actin-modulating protein cofilin is involved in the formation of measles virus ribonucleoprotein complex at the perinuclear region. *J. Virol.* 89, 10524–10531. <https://doi.org/10.1128/JVI.01819-15>.
- Krishnan, K., Moens, P.D.J., 2009. Structure and functions of profilins. *Biophys. Rev.* 1, 71–81. <https://doi.org/10.1007/s12551-009-0010-y>.
- Lamb, R.A., Parks, G.D., 2013. *Paramyxoviridae: the viruses and their replication*. In: Knipe, D.M., Howley, P.M., Cohen, J.I., Griffin, D.E., Lamb, R.A., Martin, M.A., Racaniello, V.R., Roizman, B. (Eds.), *Fields Virology* 1, sixth ed. Lippincott Williams & Wilkins, Philadelphia, PA, pp. 957–995.
- Lambrechts, A., Braun, A., Jonckheere, V., Aszodi, A., Lanier, L.M., Robbens, J., Van Colen, I., Vandekerckhove, J., Fässler, R., Ampe, C., 2000. Profilin II is alternatively spliced, resulting in profilin isoforms that are differentially expressed and have distinct biochemical properties. *Mol. Cell. Biol.* 20, 8209–8219.
- Lassing, I., Lindberg, U., 1985. Specific interaction between phosphatidylinositol 4,5-bisphosphate and profilactin. *Nature* 314, 472–474.
- Liu, G., Xiang, Y., Guo, C., Pei, Y., Wang, Y., Kitazato, K., 2014. Cofilin-1 is involved in regulation of actin reorganization during influenza A virus assembly and budding. *Biochem. Biophys. Res. Commun.* 453, 821–825. <https://doi.org/10.1016/j.bbrc.2014.10.036>.
- Nishio, M., Tsurudome, M., Kawano, M., Watanabe, N., Ohgimoto, S., Ito, M., Komada, H., Ito, Y., 1996. Interaction between nucleocapsid protein (NP) and phosphoprotein (P) of human parainfluenza virus type 2: one of the two NP binding sites on P is essential for granule formation. *J. Gen. Virol.* 77, 2457–2463. <https://doi.org/10.1099/0022-1317-77-10-2457>.
- Nishio, M., Tsurudome, M., Ito, M., Watanabe, N., Kawano, M., Komada, H., Ito, Y., 1997. Human parainfluenza virus type 2 phosphoprotein: mapping of monoclonal antibody epitopes and location of the multimerization domain. *J. Gen. Virol.* 78, 1303–1308. <https://doi.org/10.1099/0022-1317-78-6-1303>.
- Nishio, M., Tsurudome, M., Ito, M., Kawano, M., Kusagawa, S., Komada, H., Ito, Y., 1999. Mapping of domains on the human parainfluenza virus type 2 nucleocapsid protein (NP) required for NP-phosphoprotein or NP-NP interaction. *J. Gen. Virol.* 80, 2017–2022. <https://doi.org/10.1099/0022-1317-80-8-2017>.
- Nishio, M., Garcin, D., Simonet, V., Kolakofsky, D., 2002. The carboxyl segment of the mumps virus V protein associates with Stat proteins in vitro via a tryptophan-rich motif. *Virology* 300, 92–99.
- Nishio, M., Tsurudome, M., Ito, M., Garcin, D., Kolakofsky, D., Ito, Y., 2005. Identification of paramyxovirus V protein residues essential for STAT protein degradation and promotion of virus replication. *J. Virol.* 79, 8591–8601. <https://doi.org/10.1128/JVI.79.13.8591-8601.2005>.
- Nishio, M., Tsurudome, M., Ishihara, H., Ito, M., Ito, Y., 2007. The conserved carboxyl terminus of human parainfluenza virus type 2 V protein plays an important role in virus growth. *Virology* 362, 85–98. <https://doi.org/10.1016/j.virol.2006.12.017>.
- Nodelman, I.M., Bowman, G.D., Lindberg, U., Schutt, C.E., 1999. X-ray structure determination of human profilin II: a comparative structural analysis of human profilins. *J. Mol. Biol.* 294, 1271–1285.
- Ohgimoto, S., Bando, H., Kawano, M., Okamoto, K., Kondo, K., Tsurudome, M., Nishio, M., Ito, Y., 1990. Sequence analysis of P gene of human parainfluenza type 2 virus: P and cysteine-rich proteins are translated by two mRNAs that differ by two non-templated G residues. *Virology* 208, 116–123.
- Ohta, K., Goto, H., Yumine, N., Nishio, M., 2016a. Human parainfluenza virus type 2 V protein inhibits and antagonizes tetherin. *J. Gen. Virol.* 97, 561–570. <https://doi.org/10.1128/JVI.01471-16>.
- Ohta, K., Goto, H., Matsumoto, Y., Yumine, N., Tsurudome, M., Nishio, M., 2016b. Graft controls the growth of human parainfluenza virus type 2 through inactivation of RhoA signaling. *J. Virol.* 90, 9394–9405. <https://doi.org/10.1128/JVI.01471-16>.
- Ohta, K., Matsumoto, Y., Nishio, M., 2018a. Human parainfluenza virus type 2 V protein inhibits caspase-1. *J. Gen. Virol.* 99, 501–511. <https://doi.org/10.1099/jgv.0.001037>.
- Ohta, K., Matsumoto, Y., Yumine, N., Nishio, M., 2018b. The V protein of human parainfluenza virus type 2 promotes RhoA-induced filamentous actin formation. *Virology* 524, 90–96. <https://doi.org/10.1016/j.virol.2018.08.015>.
- Ohta, K., Matsumoto, Y., Nishio, M., 2018c. Rab27a facilitates human parainfluenza virus type 2 growth by promoting cell surface transport of envelope proteins. *Med. Microbiol. Immunol.* 207, 141–150. <https://doi.org/10.1007/s00430-018-0536-3>.
- Ono, S., Minami, N., Abe, H., Obinata, T., 1994. Characterization of a novel cofilin isoform that is predominantly expressed in mammalian skeletal muscle. *J. Biol. Chem.* 269, 15280–15286.
- Reed, L., Muench, H., 1938. A simple method of estimating fifty per cent endpoints. *Am. J. Epidemiol.* 27, 493–497.
- Rust, M.B., Kullmann, J.A., Witke, W., 2012. Role of the actin-binding protein profilin1 in radial migration and glial cell adhesion of granule neurons in the cerebellum. *Cell Adhes. Migrat.* 6, 13–17. <https://doi.org/10.4161/cam.19845>.
- Schutt, C.E., Myslik, J.C., Rozycki, M.D., Goonesekere, N.C., Lindberg, U., 1993. The structure of crystalline profilin-beta-actin. *Nature* 365, 810–816. <https://doi.org/10.1038/365810a0>.
- Takei, D., Ishihara, H., Yamaguchi, S., Yamada, T., Tamura, A., Maruyama, Y., Oka, Y., 2006. WFS1 protein modulates the free Ca²⁺ concentration in the endoplasmic reticulum. *FEBS Lett.* 580, 5635–5640. <https://doi.org/10.1016/j.febslet.2006.09.007>.
- Watanabe, N., Madaule, P., Reid, T., Ishizaki, T., Watanabe, G., Kakizuka, A., Saito, Y., Nakao, K., Jockusch, B.M., Narumiya, S., 1997. p140mDia, a mammalian homolog of *Drosophila* diaphanous, is a target protein for Rho small GTPase and is a ligand for profilin. *EMBO J.* 16, 3044–3056. <https://doi.org/10.1093/emboj/16.11.3044>.
- Watanabe, N., Kato, T., Fujita, A., Ishizaki, T., Narumiya, S., 1999. Cooperation between mDia1 and ROCK in Rho-induced actin reorganization. *Nat. Cell Biol.* 1, 136–143. <https://doi.org/10.1038/11056>.
- Witke, W., Podtelejnikov, A.V., Di Nardo, A., Sutherland, J.D., Gurniak, C.B., Dotti, C., Mann, M., 1998. In mouse brain profilin I and profilin II associate with regulators of the endocytic pathway and actin assembly. *EMBO J.* 17, 967–976. <https://doi.org/10.1093/emboj/17.4.967>.
- Witke, W., Sutherland, J.D., Sharpe, A., Arai, M., Kwiatkowski, D.J., 2001. Profilin I is essential for cell survival and cell division in early mouse development. *Proc. Natl. Acad. Sci. U.S.A.* 98, 3832–3836. <https://doi.org/10.1073/pnas.051515498>.
- Zan, J., An, S.T., Mo, K.K., Zhou, J.W., Liu, J., Wang, H.L., Yan, Y., Liao, M., Zhou, J.Y., 2016. Rabies virus inactivates cofilin to facilitate viral budding and release. *Biochem. Biophys. Res. Commun.* 477, 1045–1050. <https://doi.org/10.1016/j.bbrc.2016.07.030>.